Second Order Optical Nonlinearity in Glassy Material and Some Applications

清華大學電機系
趙　煦 教授
12/08/2004

- Basic Concept of Nonlinear Optics
- Phase-Matching
- Quasi-Phase-Matching (QPM)
- QPM-SHG of Blue Light in Nonlinear Crystal
- Creating Second Order Nonlinearity in Glass
- How to Implement QPM in Glass
- QPM-SHG in Glass

Some Basics of Nonlinear Optics

Hook's Law $F = kx$

or

$$x = \frac{1}{k} F$$

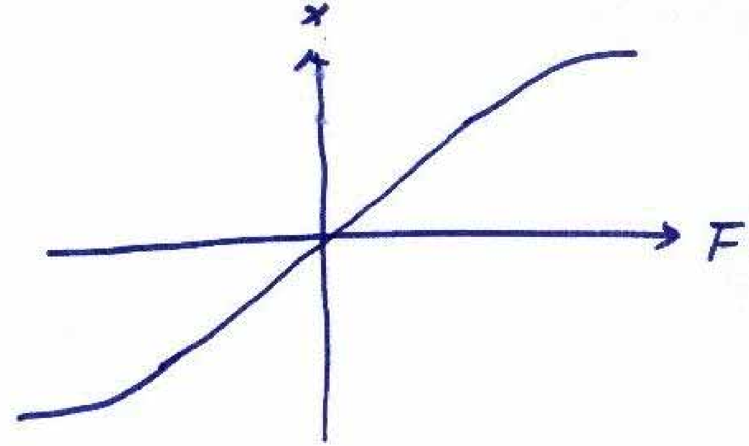

In case of nonlinearity : $k(F)$

Dielectric response : $\vec{P} = \chi(\vec{E})\,\vec{E}$

$$\vec{P} = \chi^{(0)}\vec{E} + \chi^{(2)}\vec{E}\vec{E} + \chi^{(3)}\vec{E}\vec{E}\vec{E} + \cdots\cdots$$

$$P_i = \sum_j \chi^{(0)}_{ij} E_j + \sum_j \sum_k \chi^{(2)}_{ijk} E_j E_k$$

$$+ \sum_j \sum_k \sum_l \chi^{(3)}_{ijkl} E_j E_k E_l + \cdots\cdots$$

$i, j, k, l = 1, 2, 3.$ or x, y, z.

Linear Case: $\vec{P} = \chi \vec{E}$

$$P_i = \sum_j \chi_{ij}^{(0)} E_j$$

$$\vec{P}(\vec{r}, t) = \chi(\vec{r}, t)\, \vec{E}(\vec{r}, t) \qquad ???$$

$$P_i(\vec{r}, t) = \sum_j \chi_{ij}^{(0)}(\vec{r}, t)\, \vec{E}_j(\vec{r}, t)$$

For lossy material and non-local interaction:

$$P_i(\vec{r}, t) = \sum_j \iint \chi_{ij}^{(0)}(\vec{r}-\vec{r}', t-t')\, E_j(\vec{r}', t')\, d\vec{r}'\, dt', \quad \begin{matrix} t' > t \\ \chi = 0 \end{matrix}$$

For lossy material and non-local interaction:

$$P_i(\vec{r}, t) = \sum_j \iint \chi_{ij}^{(0)}(\vec{r}-\vec{r}', t-t')\, E_j(\vec{r}', t')\, d\vec{r}'dt', \quad \begin{matrix}\chi = 0 \\ \text{when } t' > t\end{matrix}$$

Fourier transform both sides $\quad \vec{r} \to \vec{k}$

$\quad t \to \omega$

From convolution theorem: $\left(f(t) = \int h(t-t')\, g(t')\, dt' \Rightarrow F(\omega) = H(\omega) G(\omega) \right)$

$$P_i(\vec{k}, \omega) = \sum_j \chi_{ij}^{(0)}(\vec{k}, \omega)\, E_j(\vec{k}, \omega)$$

$$\left(\quad \vec{P}_i(\vec{k}, \omega) = \chi^{(0)}(\vec{k}, \omega)\, \vec{E}(\vec{k}, \omega) \quad \right)$$

Same for nonlinear case:

$$P_i(\vec{r},t) = \sum_j \chi^{(1)}_{ij}(\vec{r}-\vec{r}', t-t')\, E_j(\vec{r}',t') + \sum_j \sum_k \chi^{(2)}_{ijk}(\vec{r}-\vec{r}', \vec{r}-\vec{r}'', t-t', t-t'')\, E_j(\vec{r}',t')\, E_k(\vec{r}'',t'')$$

$$+ \sum_j \sum_k \sum_l \chi^{(3)}_{ijkl}(\vec{r}-\vec{r}', \vec{r}-\vec{r}'', \vec{r}-\vec{r}''', t-t', t-t'', t-t''')\, E_j(\vec{r}',t')\, E_k(\vec{r}'',t'')\, E_l(\vec{r}''',t''')$$

Fourier transform both sides: (with convolution theorem)

$$P_i(\vec{k},\omega) = \sum_j \chi^{(1)}_{ij}(\vec{k},\omega)\, E_j(\vec{k},\omega) + \sum_j \sum_k \chi^{(2)}_{ijk}(\vec{k}=\vec{k}_1+\vec{k}_2, \omega=\omega_1+\omega_2)\, E_j(\vec{k}_1,\omega_1)\, E_k(\vec{k}_2,\omega_2)$$

$$+ \sum_j \sum_k \sum_l \chi^{(3)}_{ijkl}(\vec{k}=\vec{k}_1+\vec{k}_2+\vec{k}_3, \omega=\omega_1+\omega_2+\omega_3)\, E_j(\vec{k}_1,\omega_1)\, E_k(\vec{k}_2,\omega_2)\, E_l(\vec{k}_3,\omega_3)$$

$$\vec{P}(\vec{k},\omega) = \chi^{(1)}(\vec{k},\omega)\, \vec{E}(\vec{k},\omega) + \chi^{(2)}(\vec{k}=\vec{k}_1+\vec{k}_2, \omega=\omega_1+\omega_2)\, \vec{E}(\vec{k}_1,\omega_1)\, \vec{E}(\vec{k}_2,\omega_2)$$

$$+ \chi^{(3)}(\vec{k}=\vec{k}_1+\vec{k}_2+\vec{k}_3, \omega=\omega_1+\omega_2+\omega_3)\, \vec{E}(\vec{k}_1,\omega_1)\, \vec{E}(\vec{k}_2,\omega_2)\, \vec{E}(\vec{k}_3,\omega_3)$$

For central-symmetric material

i.e. χ remains the same when $\vec{r} \longrightarrow -\vec{r}$

$$\Longrightarrow \chi^{(2)} = 0$$

There is no second order nonlinear effect for material with central-symmetry.

phase Matching

Example : second harmonic generation (SHG)

$$\vec{P}^{(2)}(\vec{k}=\vec{k}_1+\vec{k}_2, \omega=\omega_1+\omega_2) = \chi^{(2)}(\vec{k},\omega)\, \vec{E}(\vec{k}_1,\omega_1)\, \vec{E}(\vec{k}_2,\omega_2)$$

For SHG $\qquad \omega_1 = \omega_2 \qquad \omega = 2\omega_1$

$\qquad \vec{k}_1 = \vec{k}_2 \qquad \vec{k} = 2\vec{k}_1$

$$\vec{E}_\omega \xrightarrow{\omega,\ \vec{k}_\omega} \qquad v_p = \frac{\omega}{k_\omega} \qquad |\vec{k}_\omega| = \frac{2\pi n_\omega}{\lambda_\omega}$$

$$\vec{P}^{(2)} \xrightarrow{2\omega,\ 2\vec{k}_\omega} \qquad v_p = \frac{\omega}{k_\omega}$$

$$\vec{E}_{2\omega} \xrightarrow{2\omega,\ \vec{k}_{2\omega} = ?} \qquad v_p = \frac{2\omega}{k_{2\omega}} \qquad |\vec{k}_{2\omega}| = \frac{2\pi n_{2\omega}}{\lambda_{2\omega}}$$

phase matching between $\vec{P}^{(2)}$ and $\vec{E}_{2\omega}$: $\vec{k}_{2\omega} = 2\vec{k}_\omega$

$$\Longrightarrow n_\omega = n_{2\omega}$$

in phase matched : $\Delta\vec{k} = \vec{k}_{2\omega} - 2\vec{k}_\omega = 0$

SHG Power Conversion

$$\eta = \frac{P_{2\omega}}{P_\omega} = 2\left(\frac{\mu}{\varepsilon_0}\right)^{\frac{3}{2}} \cdot \frac{\omega^2 d_{eff}^2}{n_\omega^2 n_{2\omega}} \cdot \sin c^2\left(\frac{\Delta kL}{2}\right) \cdot \frac{L^2 P_\omega}{A}$$

$$\Delta k = k_{2\omega} - 2k_\omega$$

$$l_c = \frac{2\pi}{\Delta k} = \frac{\lambda}{4(n_{2\omega} - n_\omega)}$$

coherence length

SHG in Waveguide

$$k_\omega \to \beta_\omega^p$$

$$k_{2\omega} \to \beta_{2\omega}^q$$

$$\frac{1}{A} \to (overlap\ integral)^2$$

$$= \left[\iint E_{2\omega}^q \cdot E_\omega^p E_\omega^{p*} dxdy\right]^2$$

Quasi-Phase-Matching

Historical

– 1962 Armstrong, Bloembergen, Ducning, Pershan
Phys. Rev. 127, 1918

$$\vec{P}(\omega_3) = \varepsilon_0 \ \overline{\overline{\chi}}^{(2)} : \vec{E}(\omega_1)\vec{E}(\omega_2)$$

$$\Delta\vec{K} = \vec{K}_3 - \vec{K}_2 - \vec{K}_1 + \frac{2\pi}{\Lambda}\hat{k} = 0$$

$$\Lambda : periode \ of \ \ periodical \ reversal \ of \ \ \chi^{(2)}$$

Quasi-Phase-Matching (Periodic reversal of $\chi^{(2)}$)
– Periodic insertion of crystal with an inverted crystal orientation
_ Periodic reversal of ferroelectric domain of nonlinear crystal (periodic poling)

QPM-SHG in Ferroelectric Crystal

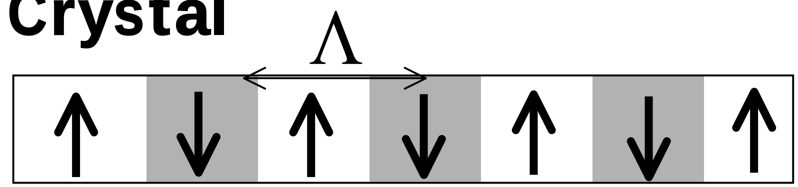

$$\frac{P_{2\omega}}{P_\omega} = \eta P_\omega L^2 \sin c^2\left(\frac{\Delta k L}{2}\right)$$

$$\eta = 8\pi^2 \left(G_m d_{eff}\right)^2 / \varepsilon_0 n_\omega^2 n_{2\omega} c \lambda_\omega^2 A$$

$$G_m = \frac{2}{\pi m} \sin\left(m\pi D\right)$$

$l_c \equiv \pi / \Delta k$: coherent length

$$\Delta k = k_{2\omega} - 2k_\omega = 2\pi / 2lc = 2\pi m / \Lambda$$

$$for\ 850nm \rightarrow 425nm \ \Rightarrow\ l_C = 1.9um$$

$$\Lambda_{1st} = 3.8\mu m\ ,\ \Lambda_{3rd} = 11.4\mu m$$

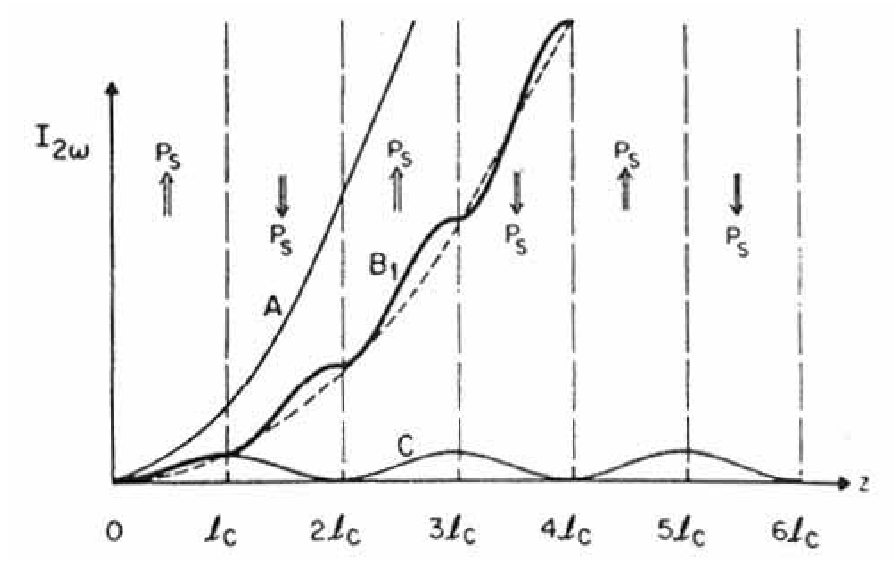

Bulk coupling

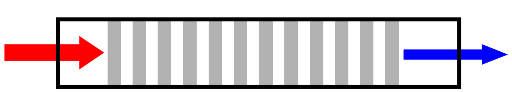

End-fire coupling to waveguide

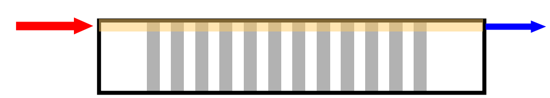

Second Harmonic Generation

$1^{st}\ \ order\ \ \Lambda_1 = 1 \times 2l_C$

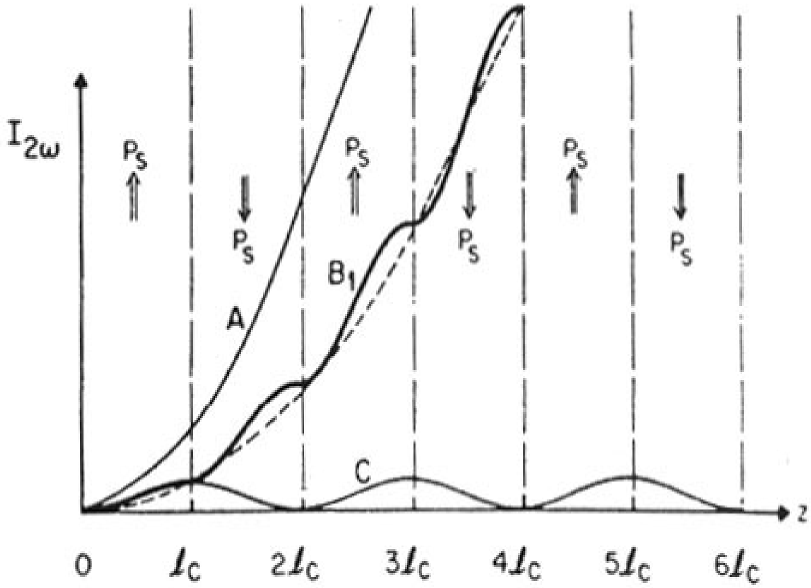

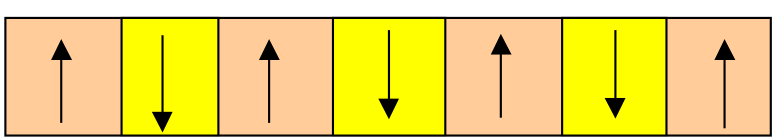

$3^{rd}\ \ order\ \ \Lambda_3 = 3 \times 2l_C$

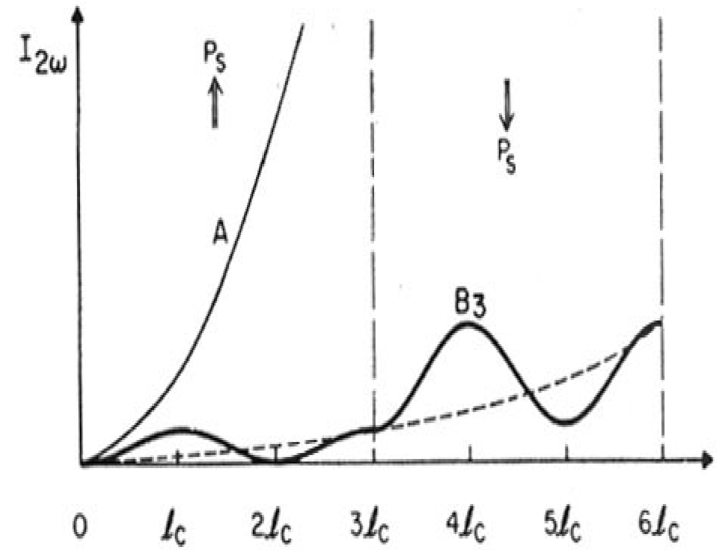

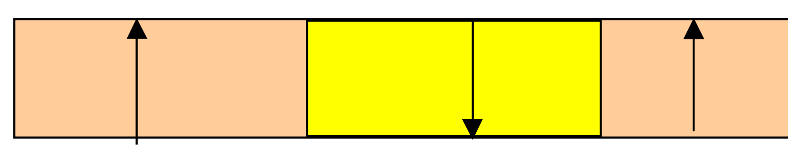

Periodic Poling

Periodic Poling of FerroElectric domain in $LiTaO_3$, $LiNbO_3$, KTP

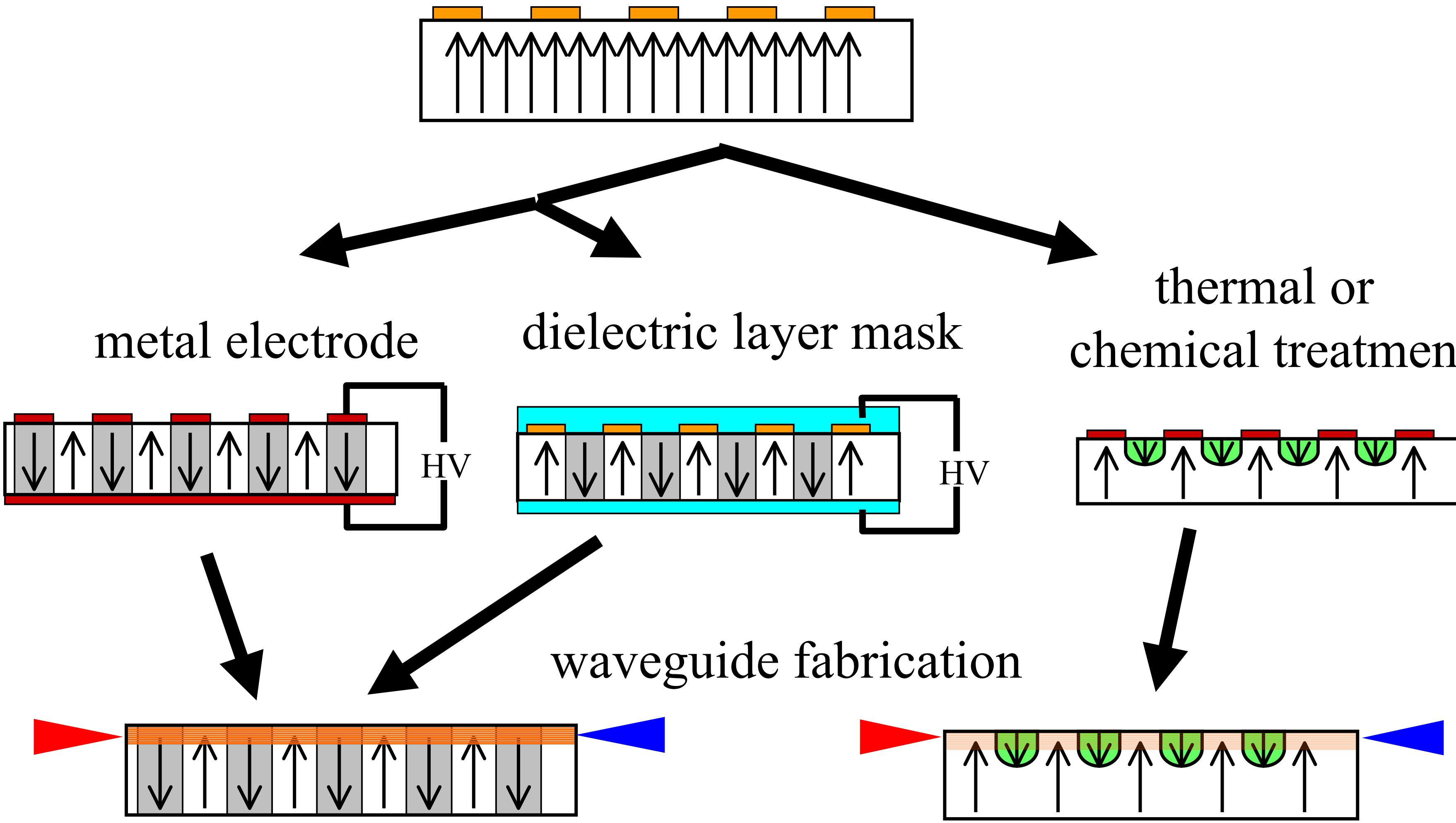

Poling apparatus

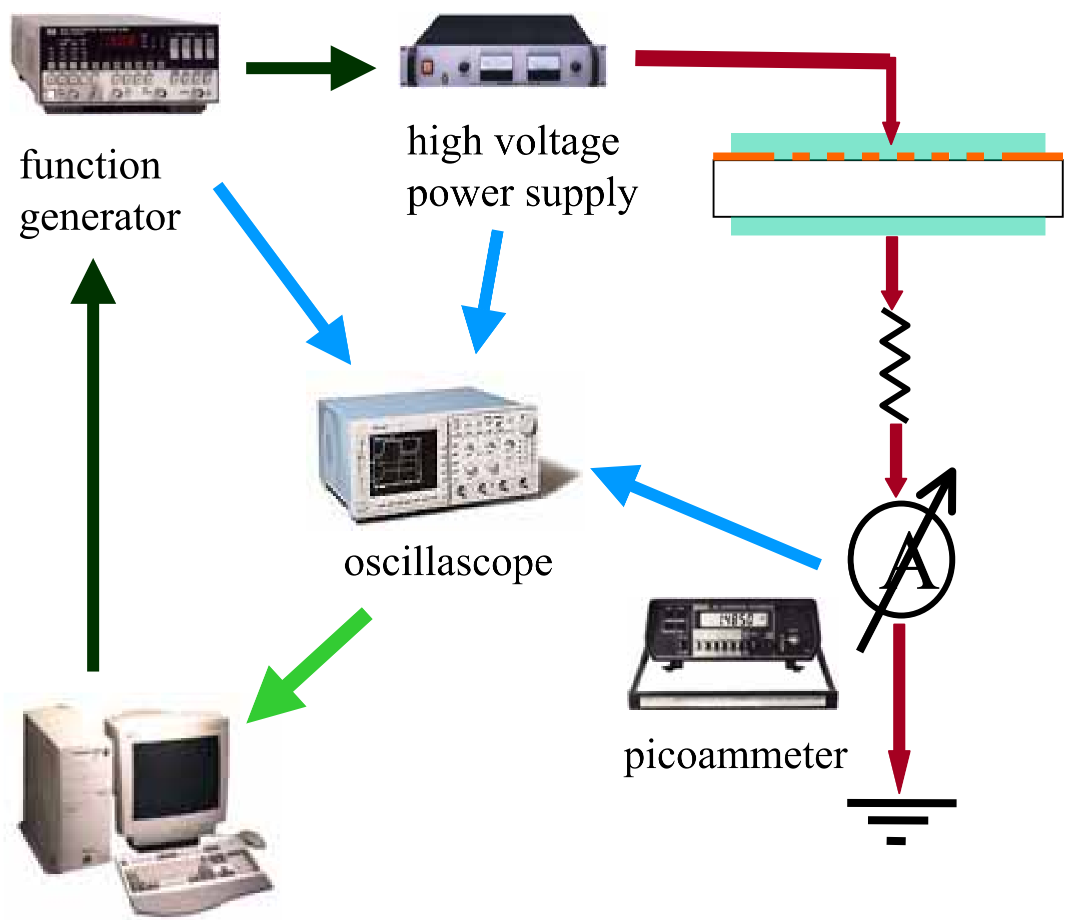

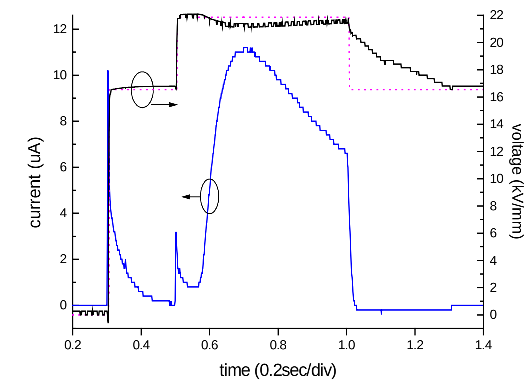

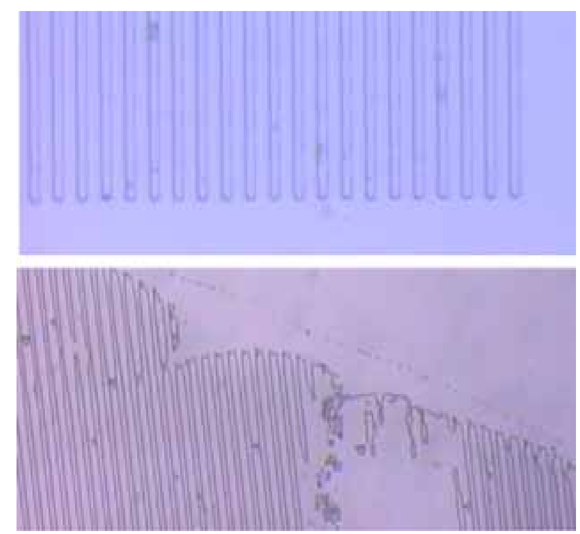

Results

Uniform, straight and precise
duty structure achieved
for 3rd QPM-SHG

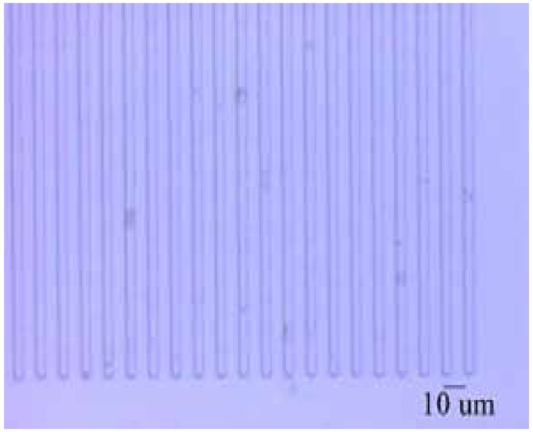

Different period structure
viewed from samples' edge

100 um 30 um 20 um 10 um

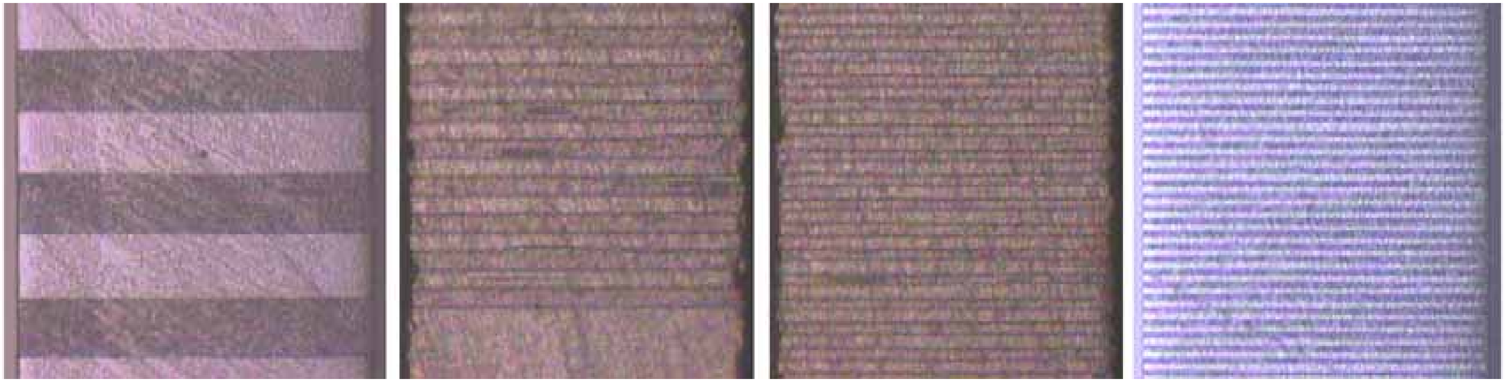

光學量測架設

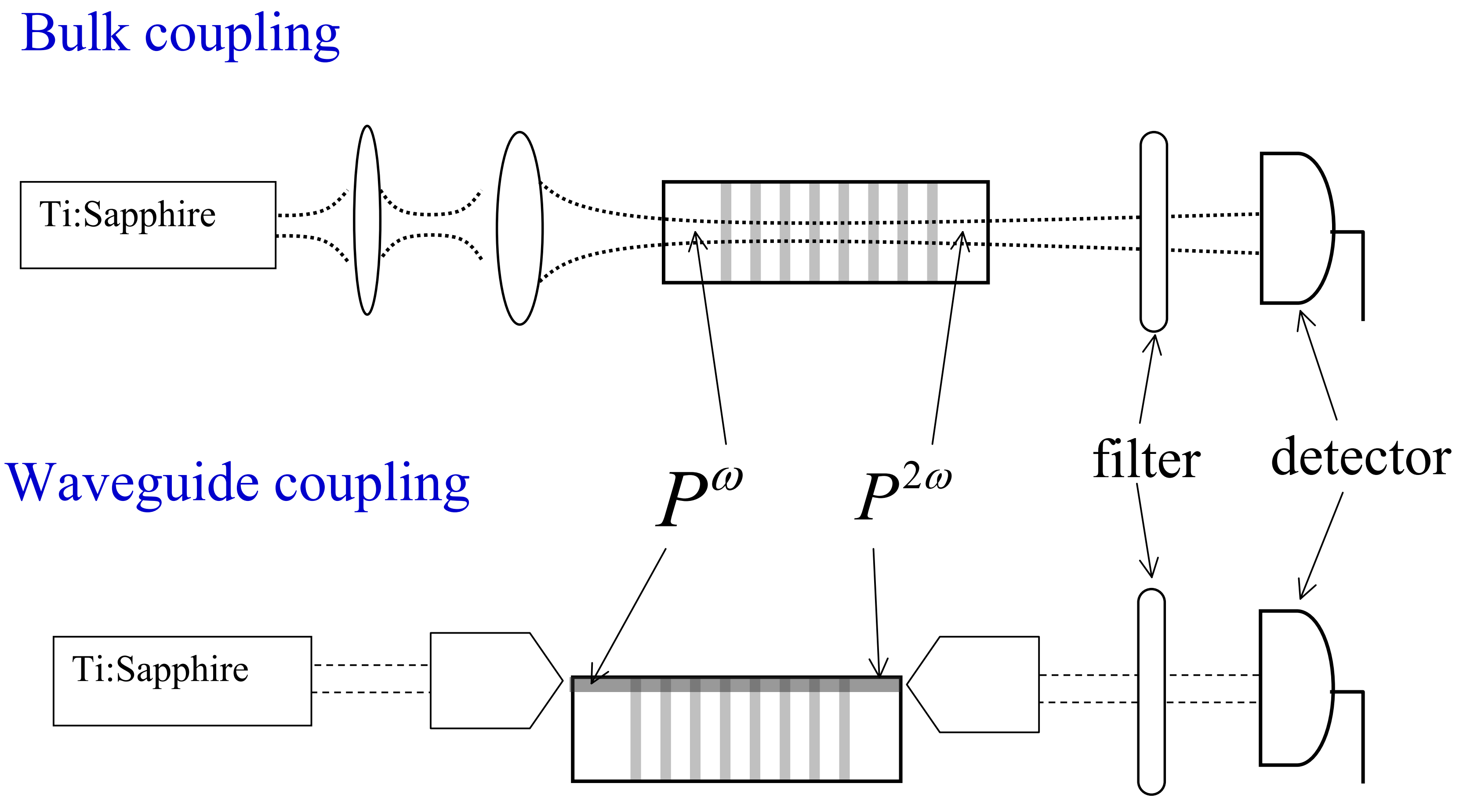
Bulk coupling
Ti:Sapphire
Waveguide coupling
P^{ω}
$P^{2\omega}$
filter
detector
Ti:Sapphire

QPM-SHG of blue light in PPLT

- Fabrication of PPLT realized
- Poling mechanism understood and QPM-SHG quality improved
- Generation of 1st (3.8um), 3rd (11.4um) order QPM-SHG blue light in bulk and in proton exchanged waveguide were achieved

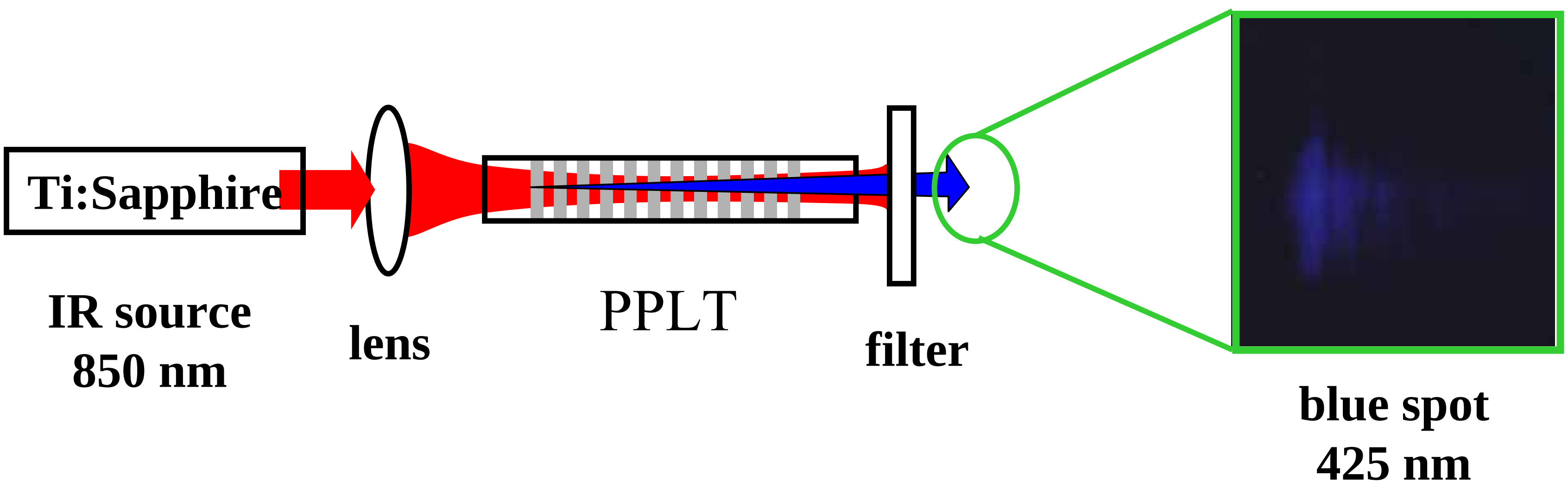

Fundamental wavelength scan

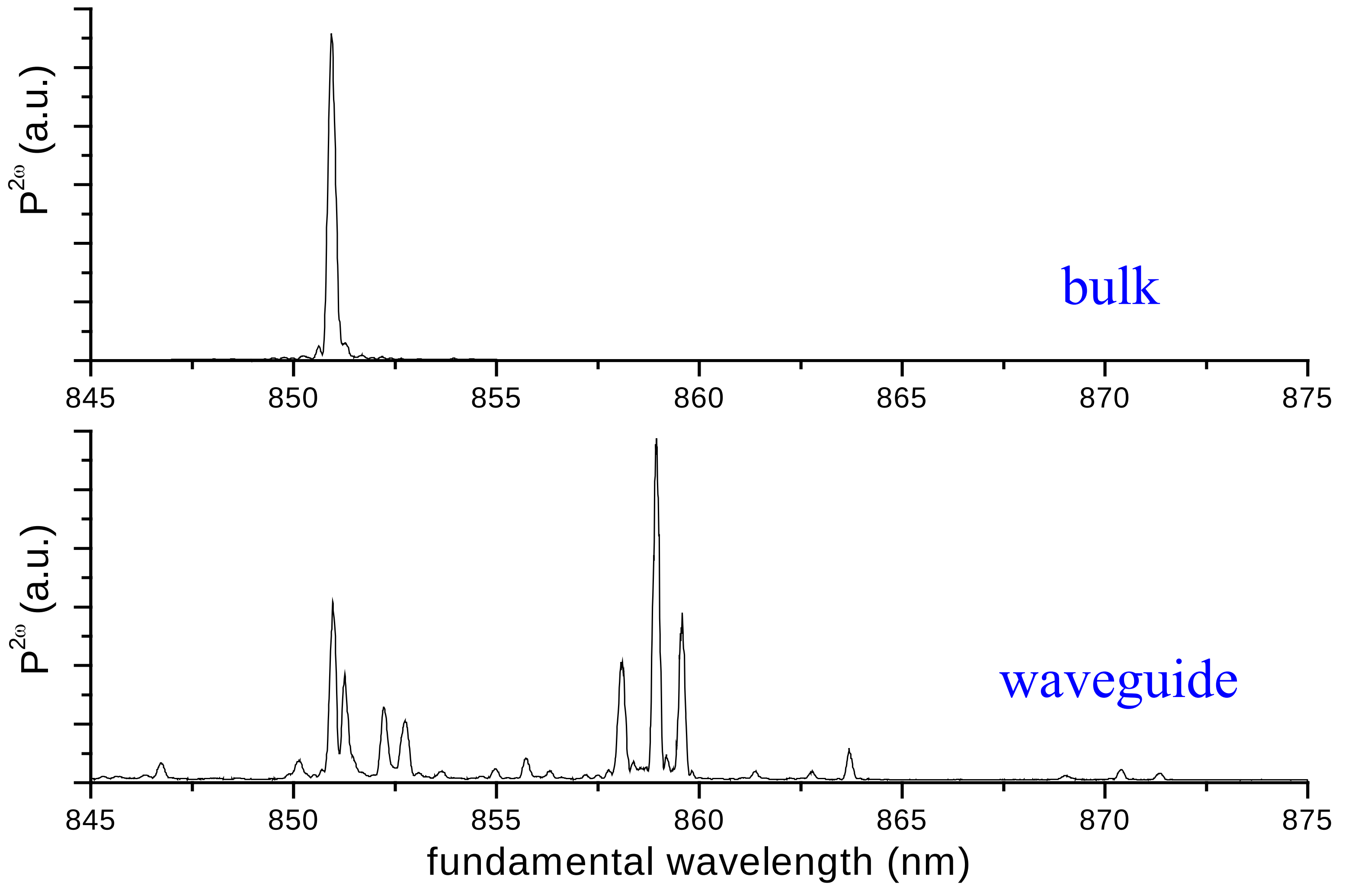

Fundamental wavelength scan

channel waveguide

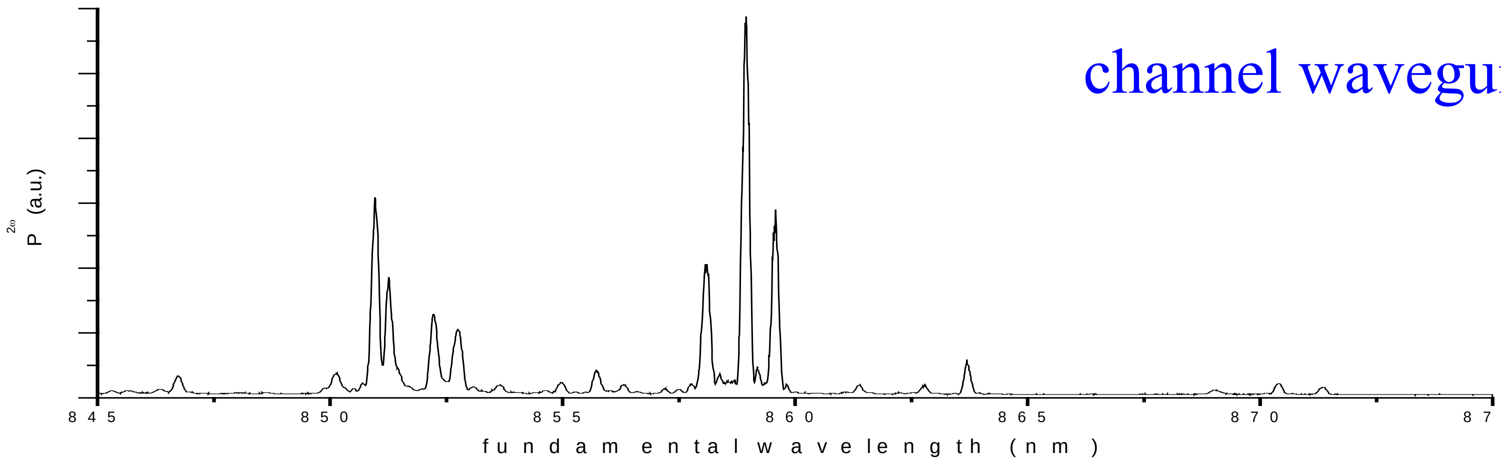

Second Order Nonlinearity in Glass Material

- P= $\chi^{(0)}$ E+ $\chi^{(2)}$ EE+ $\chi^{(3)}$ EEE+………..

- $\chi^{(2)} = 0$ for glass (centro-symmetric)

  but if $\chi^{(3)} EEE = \chi^{(3)} E_{dc}EE = \chi^{(2)} EE$

  with $\chi^{(3)} E_{dc} = \chi^{(2)}$

  E_{dc} : built-in dc field

E-field induced Mechanisms (I)

❖ **Electric-field-induced second-harmonic generation (EFISHG)**

where

for centro-symmetric medium

Creation of Built-in Field in Silica Glass : Thermal Poling

Under high Temperature and high dc voltage ,a intense electric field (E_{dc}) is established for orientation of bonds near the anode surface the.

=>depletion region of E_{dc} break centosymmetric => $\chi^{(2)} = 3\,\chi^{(3)} E_{dc}$

(1). a.single-carrier model

b.multiple-carrier model

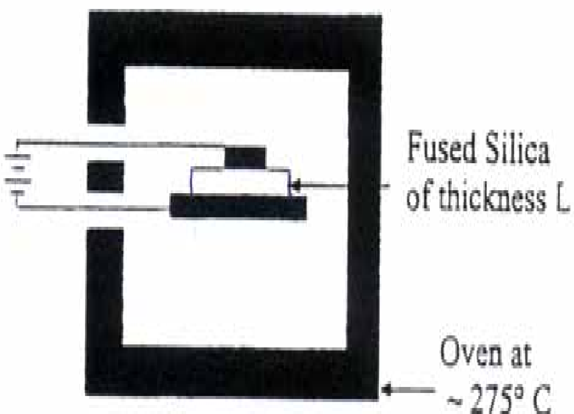

Figure 3.1 Basic poling setup

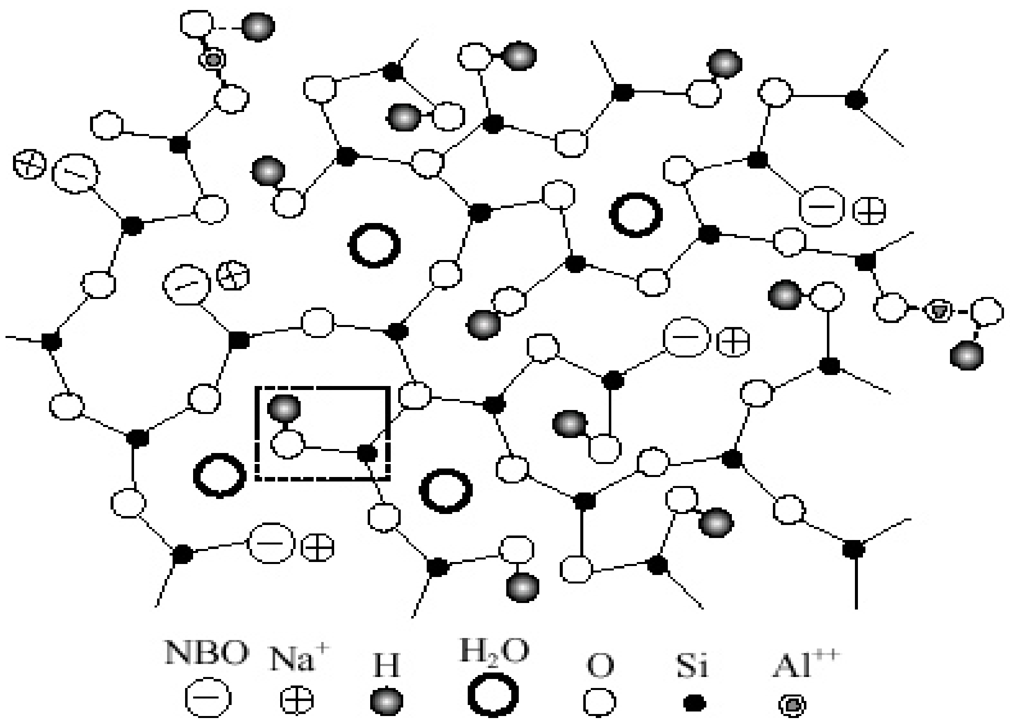

Fig. 3. Planar schematic diagram of silica network before poling.

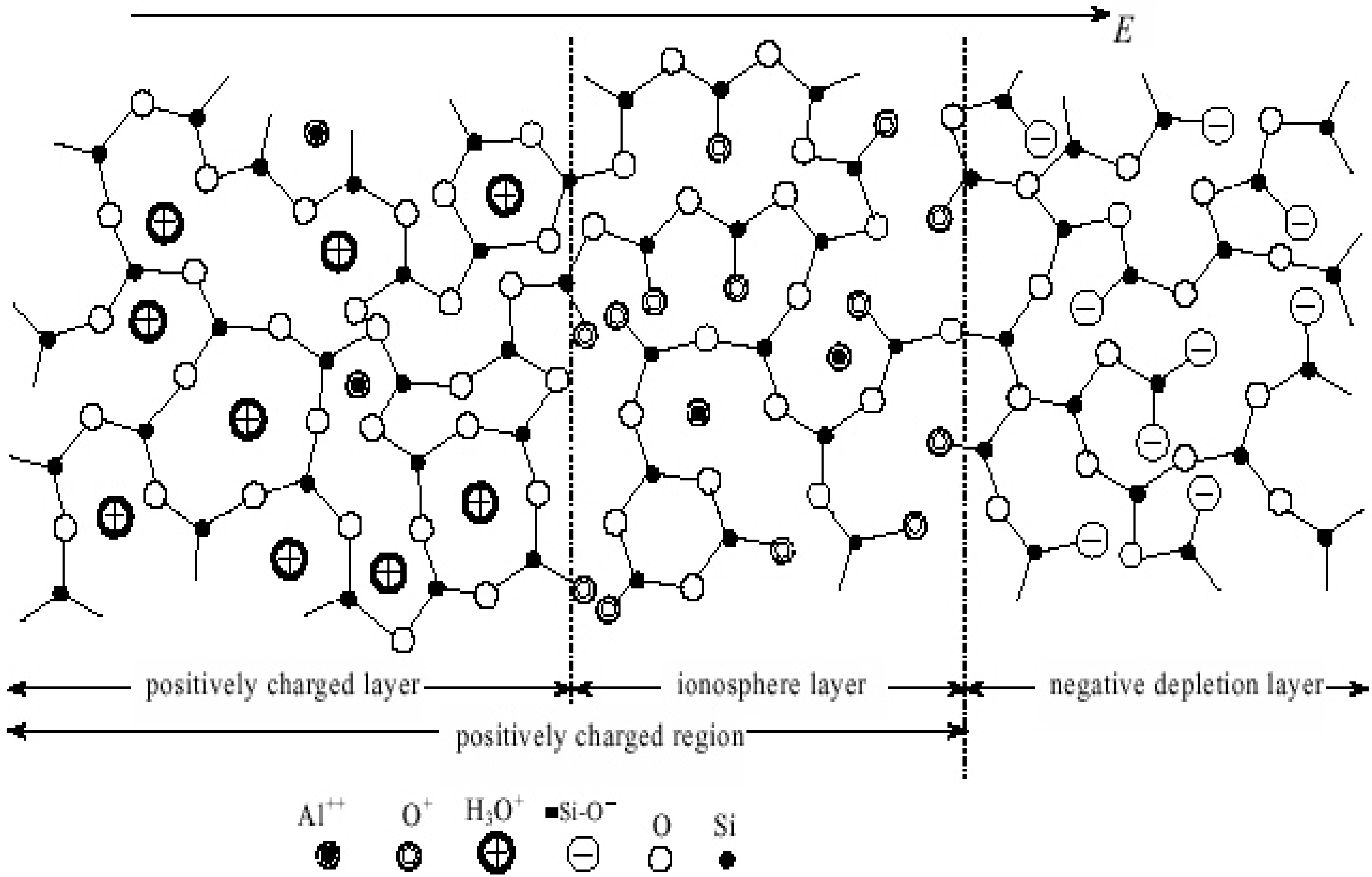

Fig. 7. Planar schematic diagram of silica network after poling.

(D)Depletion region generation process:

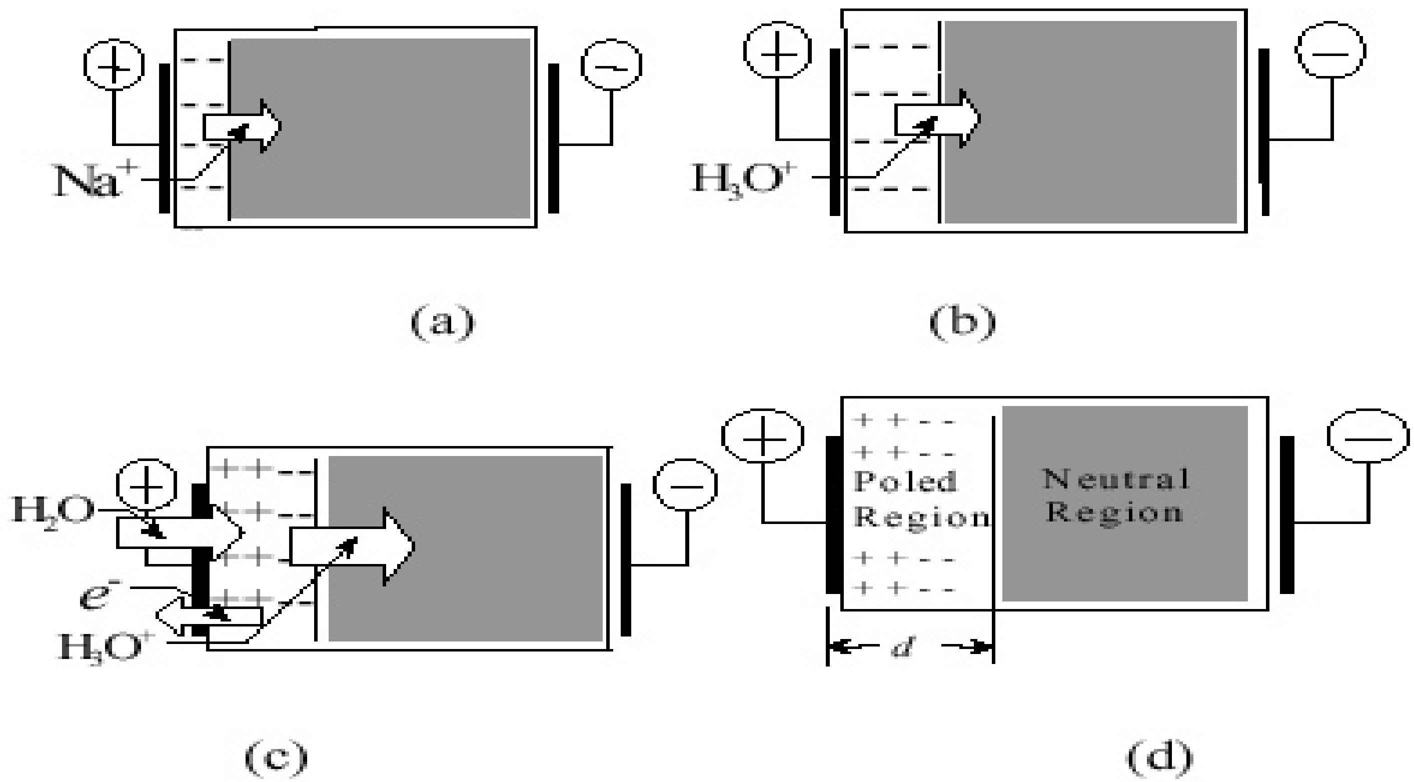

Fig. 5. Formation process of the depletion region near the anode surface in the multiple-carrier model. (a) The primary process from scores of milliseconds to several seconds in the TEFP; (b) from several seconds to scores of seconds in the TEFP; (c) after several seconds in the TEFP; (d) the state after scores of milliseconds reach the quasi-steady state.

$$\equiv Si - O - \equiv Si + H_2O \rightleftharpoons 2 \equiv Si - OH$$

$$\equiv Si - OH + H_2O \rightleftharpoons \equiv Si - O^- + H_3O^+$$

$$\equiv Si - O^- \rightleftharpoons \equiv Si - O + e^-$$

Maker fringe setup

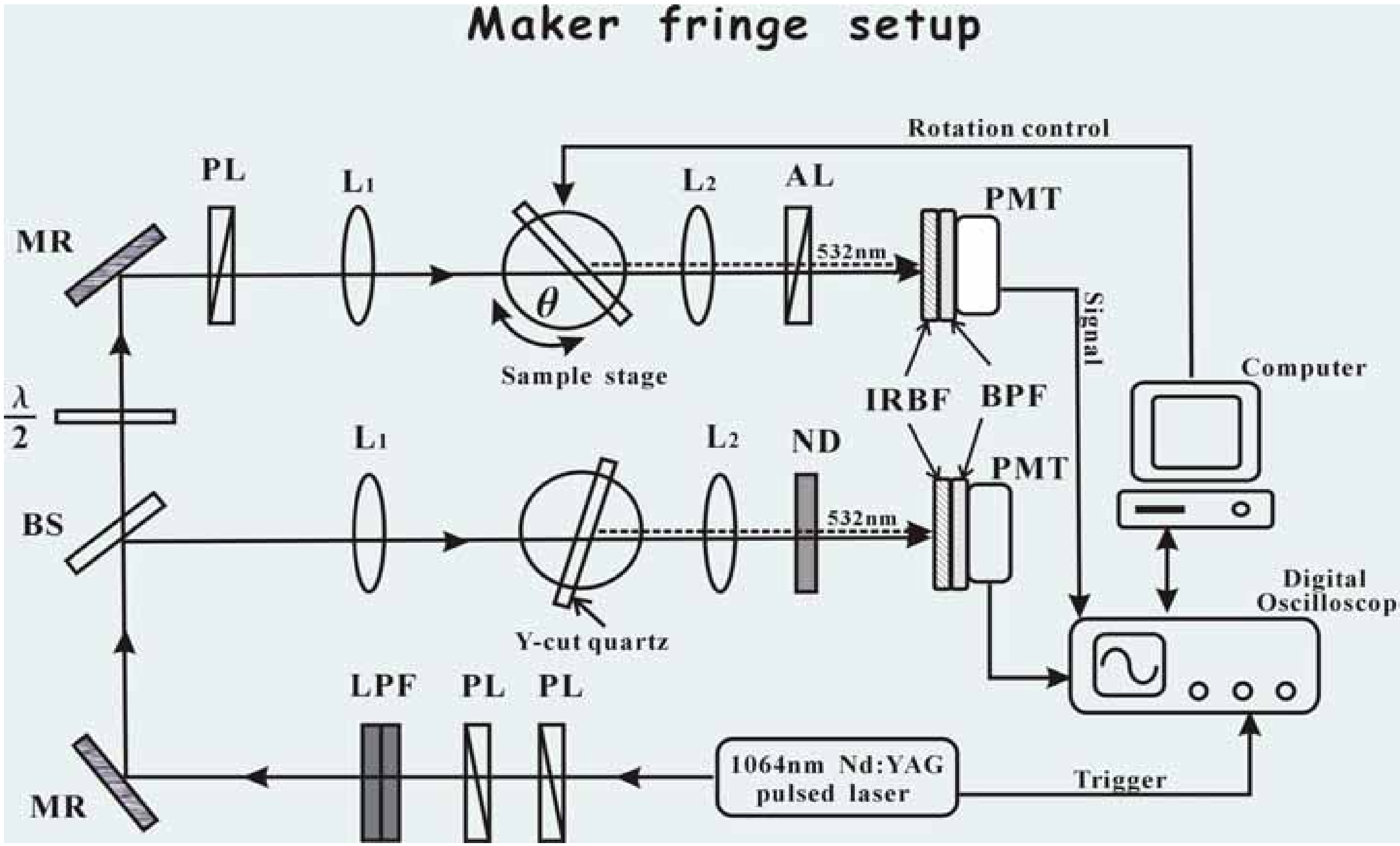

Maker fringe measurement

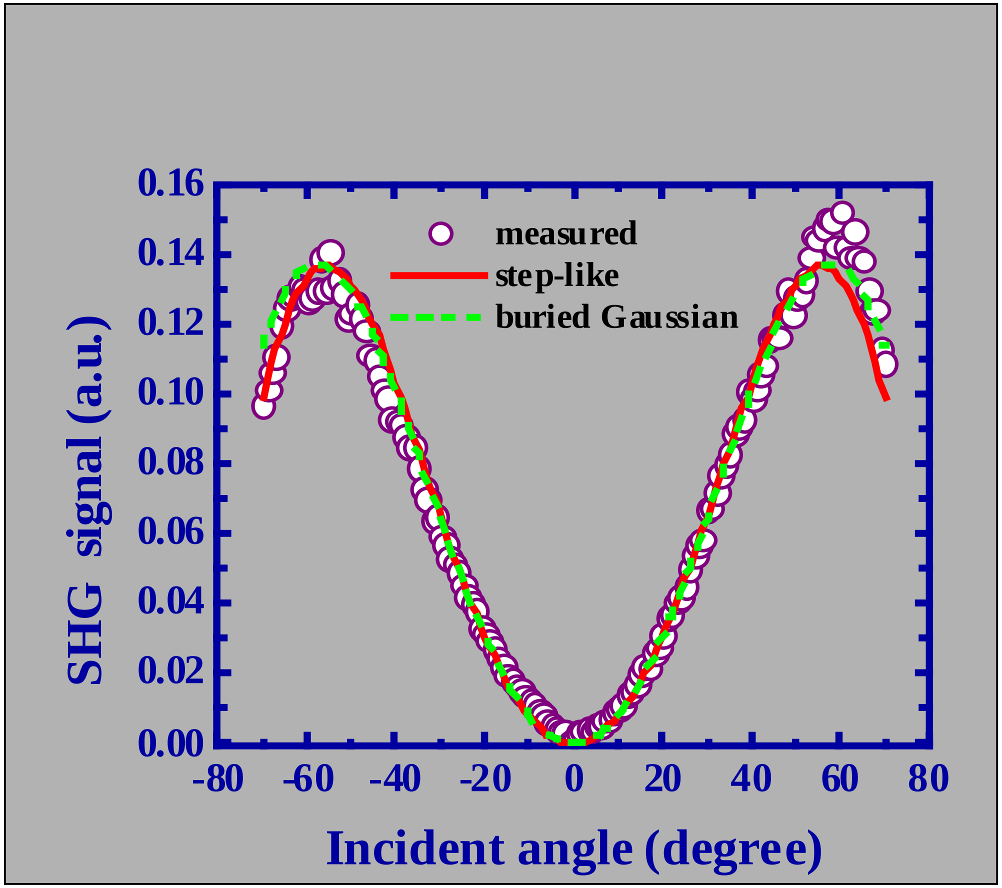

How to implement QPM in glass?

UV erasure of second-order nonlinearity

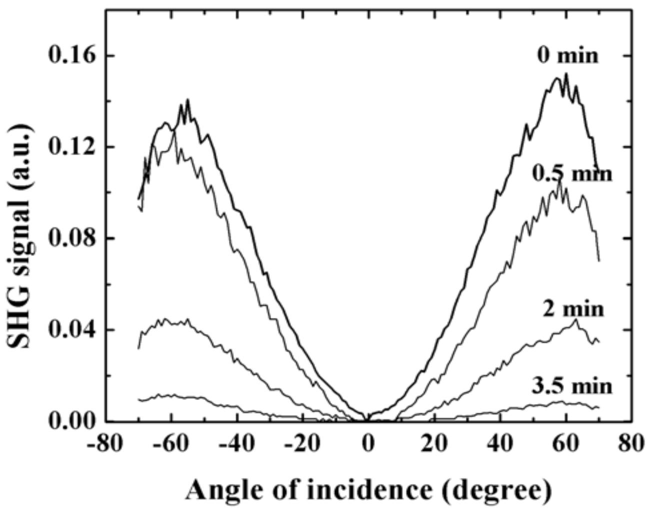

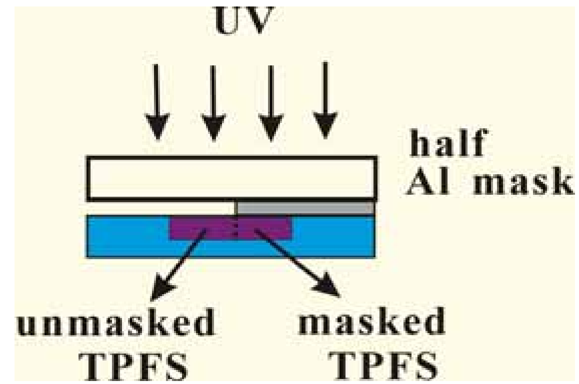

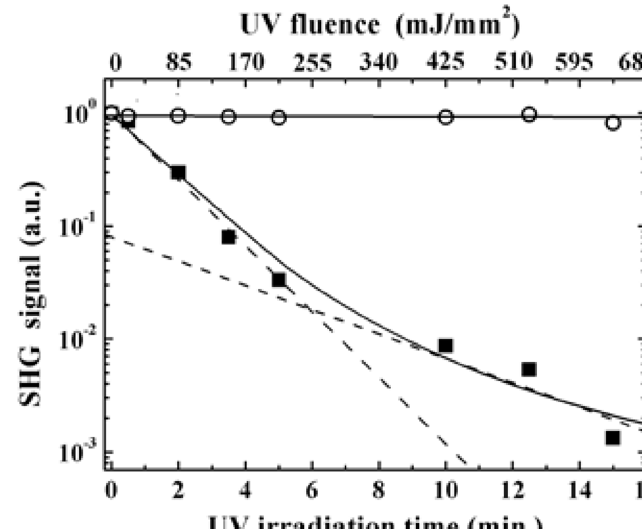

Periodic poling & etched profile

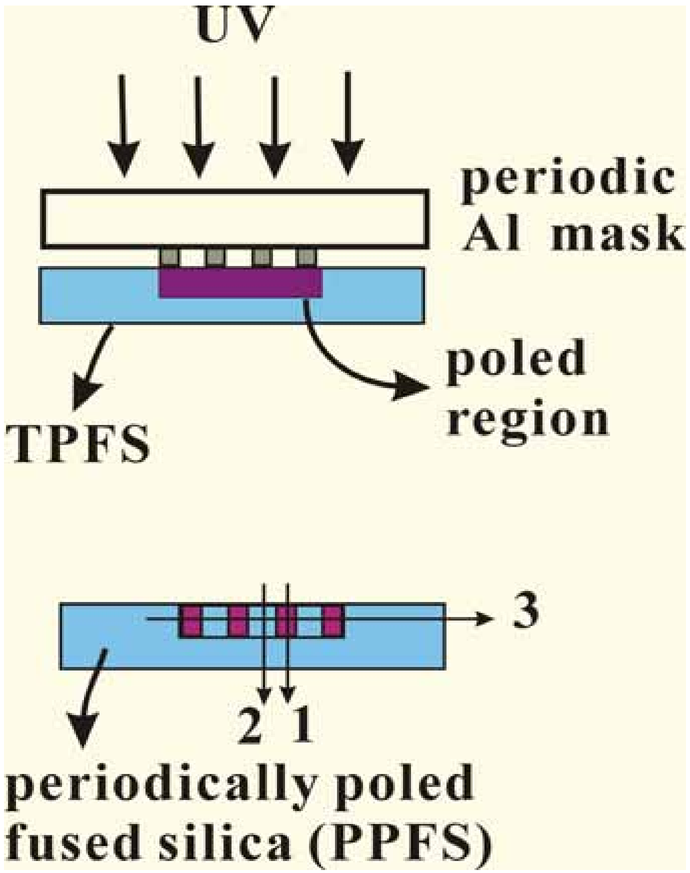

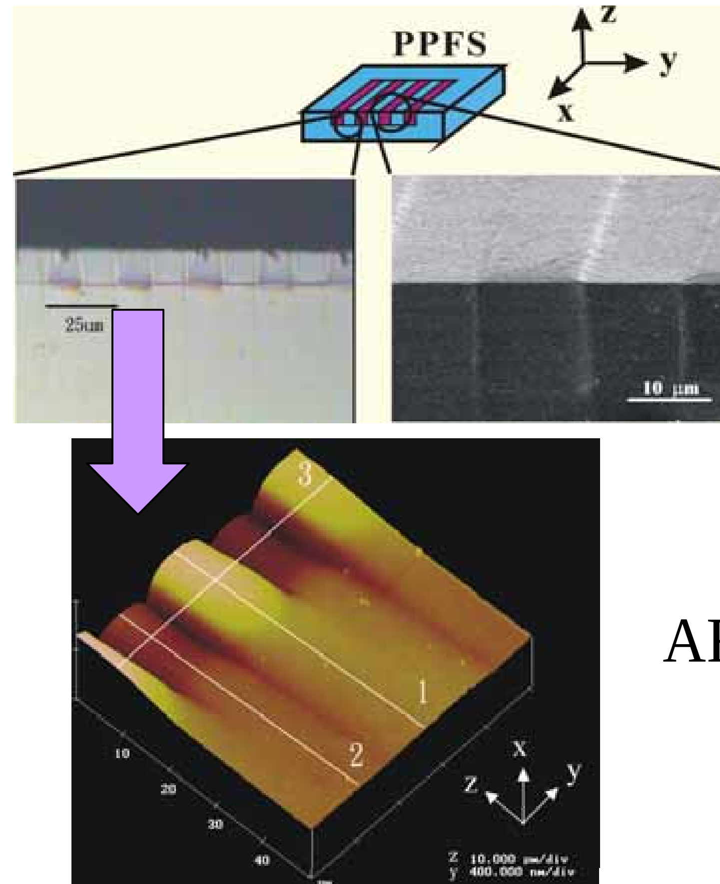

AFM

Device fabrication

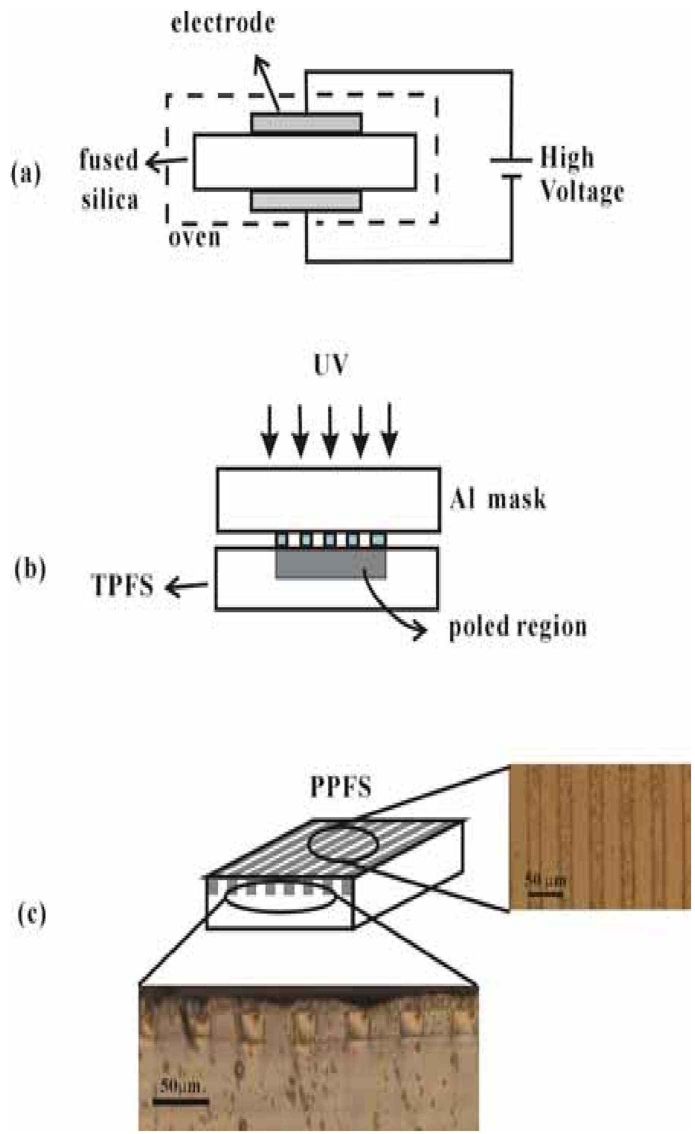

SHG test

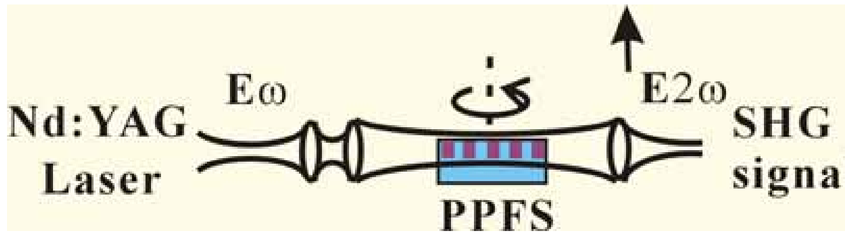

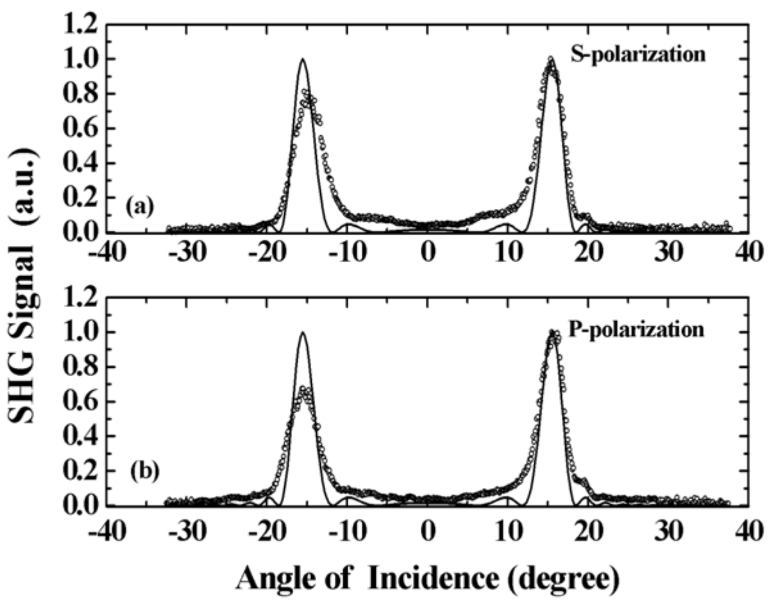

Angle tuning curve

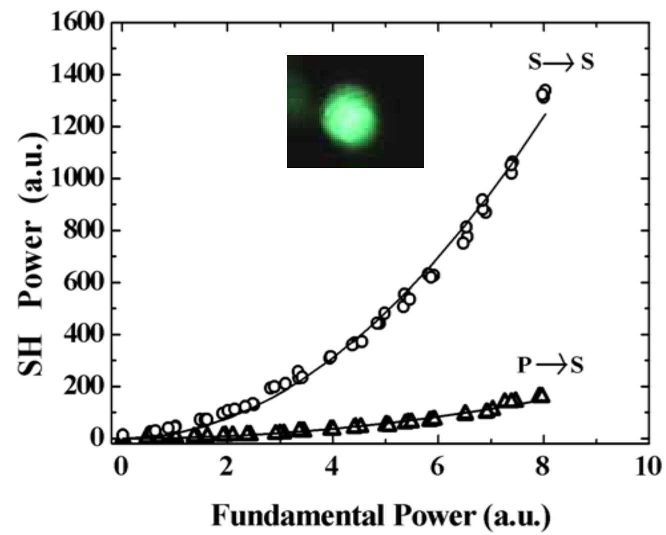

P_{2w} vs. P_w

QPM-SHG in Ge ion-implanted nonlinear optical channel waveguides

Fabrication flow chart

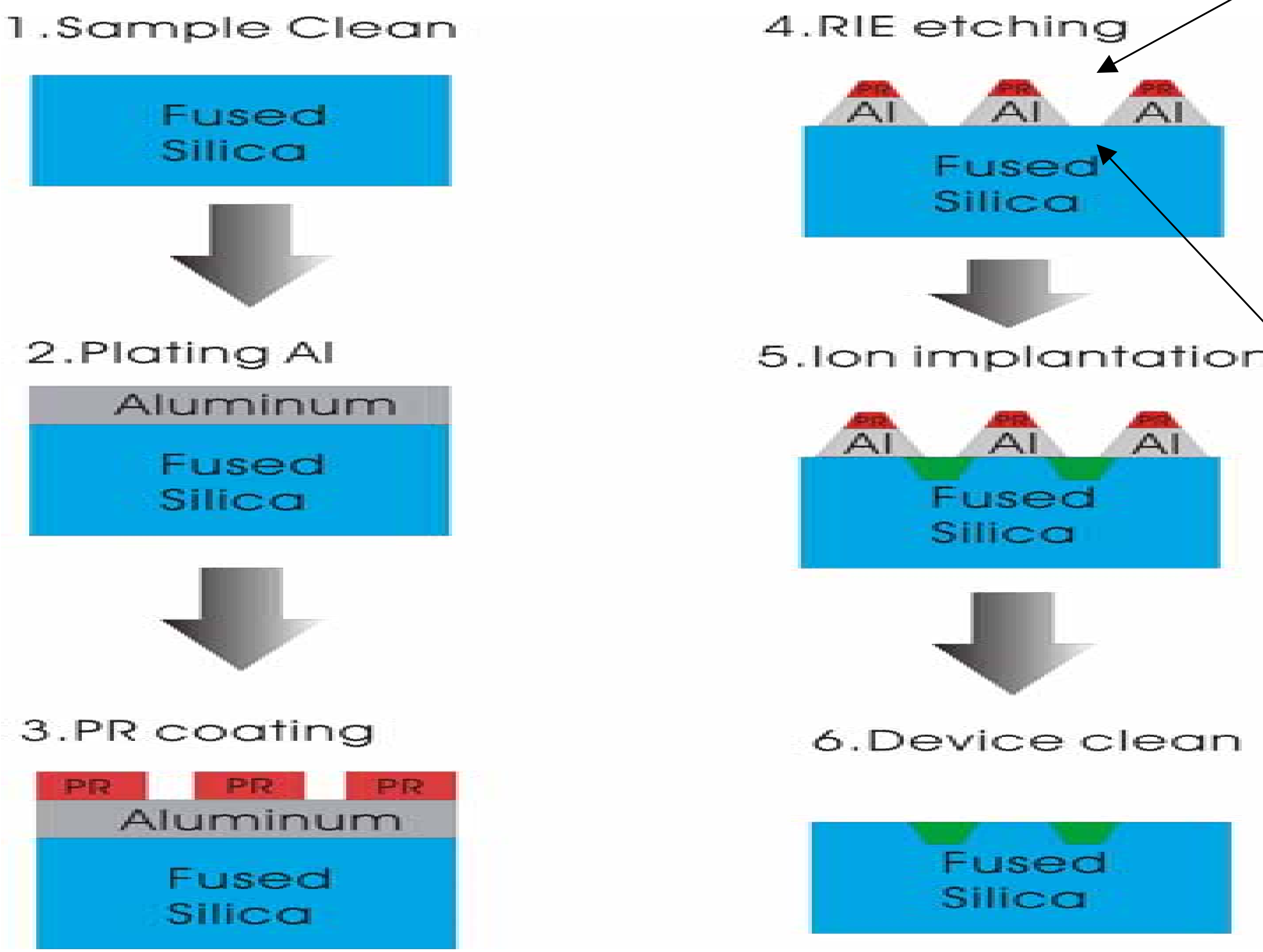

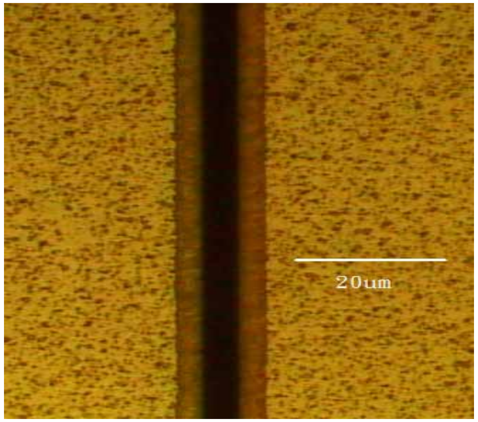

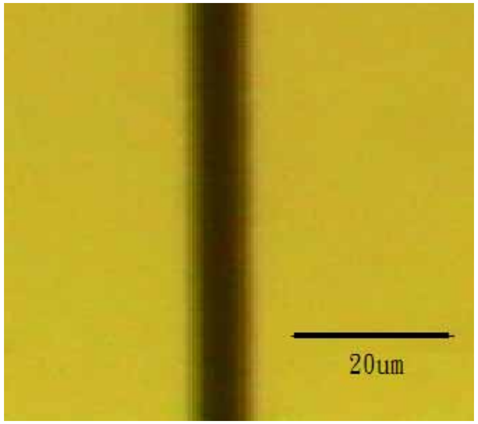

Periodical UV-erasure of second order nonlinearity

A.

UV-Erasure AL Mask

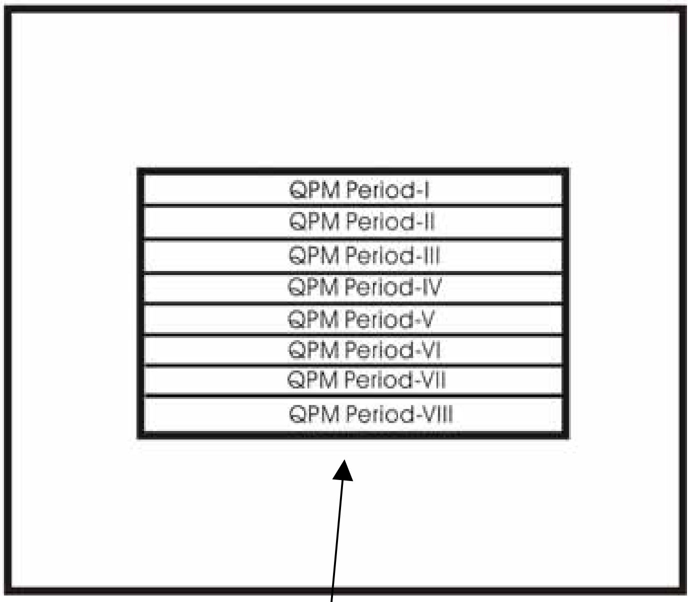

8 difference period

B.

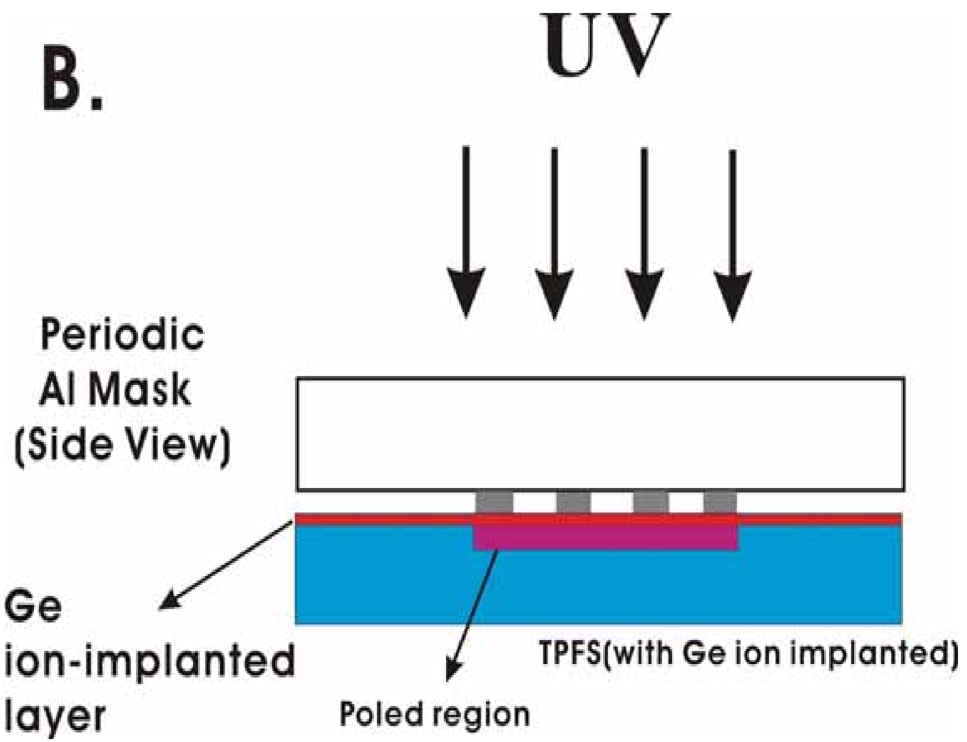

Poling & UV-erasure characteristic

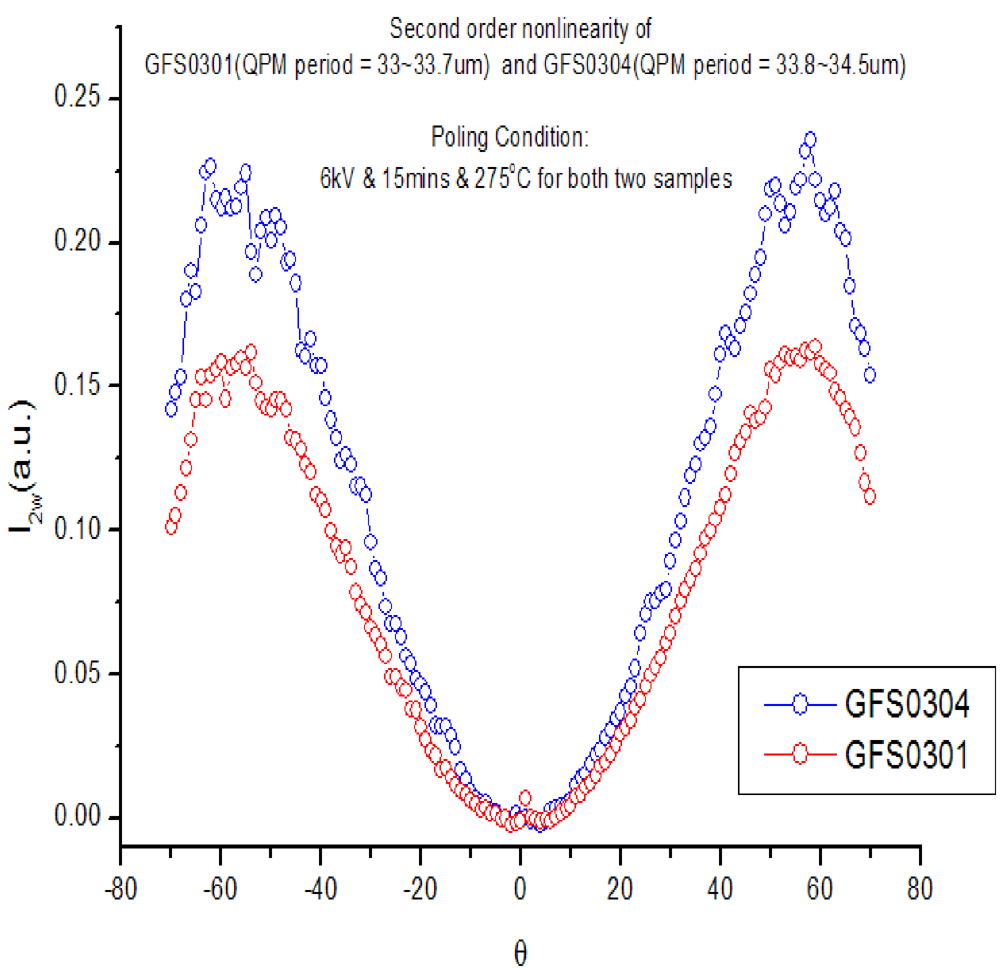

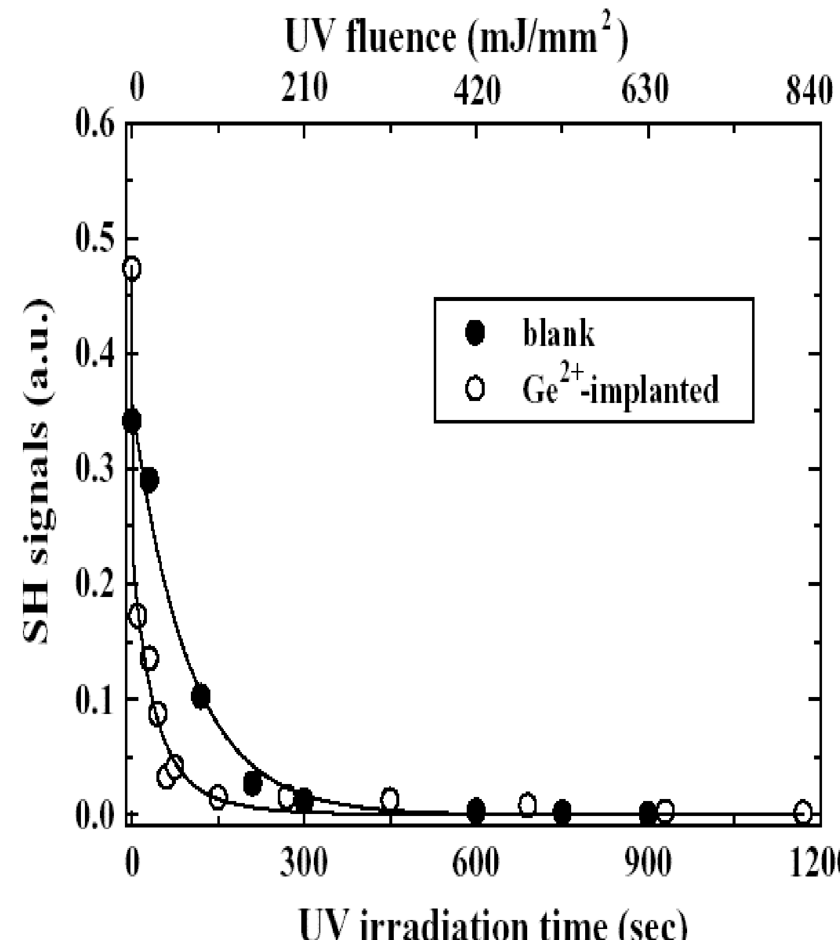

Future applications

Silica-based active device on Si wafer

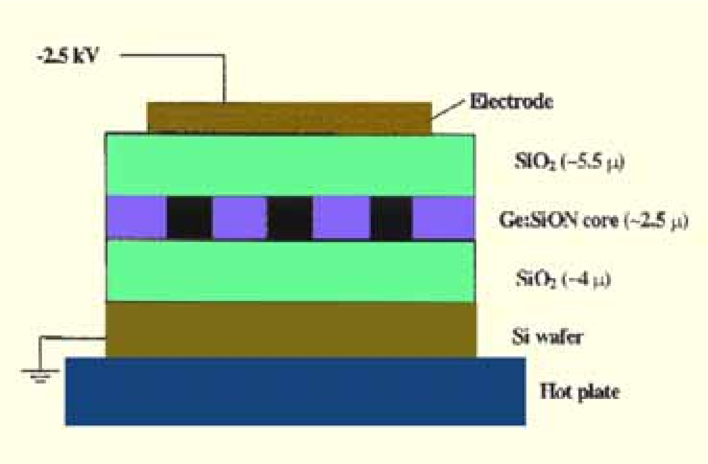

Silica-based EO device [8]

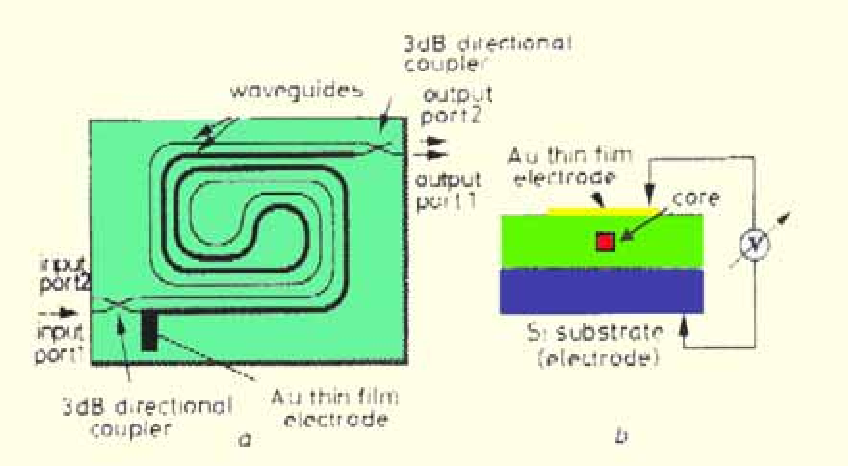

Silica-based MZ interferometer [9]

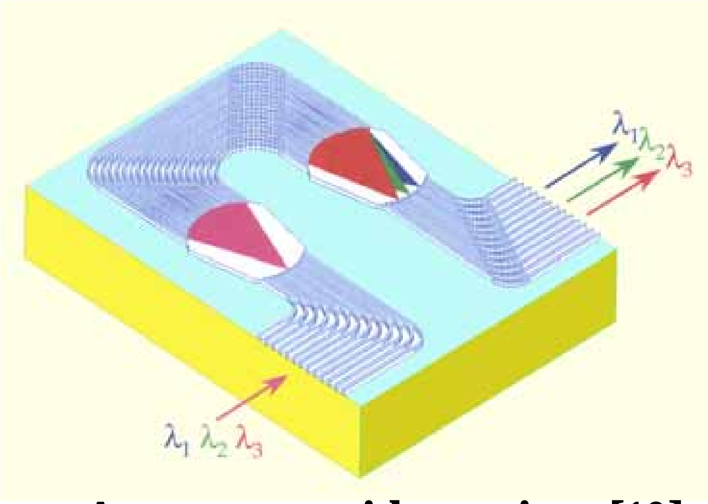

Array waveguide grating [10]

Frequency conversion device
EO modulator switch